Vol.66: e23220860, 2023
https://doi.org/10.1590/1678-4324-2023220860
ISSN 1678-4324 Online Edition

Article - Engineering, Technology and Techniques

Mathematical Modeling of Double Filtration by Colloidal Theory with Study Water Containing *Microcystis* spp.

Laís Ayumi Hataishi[1*]
https://orcid.org/0000-0001-5465-1085

Alexandre Botari[2]
https://orcid.org/0000-0002-0736-8372

[1]Universidade Estadual de Maringá, Programa de Pós-graduação em Sustentabilidade, Umuarama, Paraná, Brasil; [2]Universidade Estadual de Maringá, Programa de Pós-graduação em Sustentabilidade, Departamento de Tecnologia – DTC, Umuarama, Paraná, Brasil.

Editor-in-Chief: Alexandre Rasi Aoki
Associate Editor: Marcos Pileggi

Received: 09-Nov-2022; Accepted: 28-Jul-2023

*Correspondence: laishataishi@gmail.com; Tel.: +55-44-99709-6757 (L.A.H.)

HIGHLIGHTS

- The application of mathematical models allows the study of complex environments.
- The chemical coagulant acts on electrostatic destabilization, decreasing the absolute value of the electrical potential of the electrical double layer.
- The XDLVO theory is efficient in studying the behavior of energies and interaction forces along the particle separation distance.

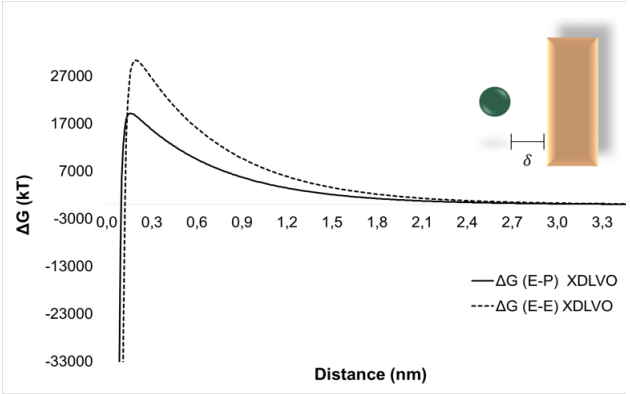

Abstract: Anthropic activities have been causing serious impacts in aquatic environments, deteriorating the quality of the waters. Superficial springs with excess of nutrients, rich in compounds of phosphor and nitrogen, may induce blooms of algae and cyanobacteria, hard to be removed in the treatment of water. Such microscopic particles, e.g. *Microcystis* spp., are named biocolloids. This work propose to apply the mathematical modelling by the extended colloidal XDLVO theory (Extended Derjarguin-Landau-Verwey-Overbeek) for coagulation and gravel upflow filtration (GUF) and sand downflow rapid filtration (SDRF) to the technology of double filtration applied to study water containing *Microcystis* spp. The XDLVO theory has been shown to be efficient at evaluating the behavior of the colloidal particles as a function of the separation distance, making apparent how the intermolecular and surface forces act: acid-base interaction (AB), Lifshitz-Vander Walls (vdW), double electric layer (DEL) and Born repulsion forces. Such forces that act in this colloidal system formed by *Microcystis* spp. were analyzed in terms of their mutual interaction and their interaction with porous environments in double filtration at the stable thermodynamic situations (pre-coagulation) and at unstabilized by the chemical coagulation. The raw water energetic barrier of repulsion and after the sand downflow rapid filtration gave an average decreasing of about 90% in absolute values.

Keywords: cyanobacteria; biocolloids; XDLVO theory.

INTRODUCTION

The water used in for public supply derives from surface water bodies or underground water wells. Surface waters go to the Water Treatment Plant (WTP) in order to attend the standard of drinking water [1], currently established in Brazil by Portaria GM/MS nº 888/2021. Due to the multiple anthropic activities, those springs may be modified, the growing of bluish green algae being of great concern for the provision of potable water [2]. In several regions the water full of algae due to the eutrophication of big lakes and reservoirs is used as raw water for drinking water [3]. The eutrophication is a phenomenon which occurs due to the high presence of nutrients in the water bodies, especially nitrogen and phosphor, favoring the excessive increase of micro algae, what turns out to be deleterious to aquatic ecosystems [4,5].

Eutrophicated environments have water with high turbidity, characterized in several cases by the excessive presence of suspended colloidal particles. Such particles can be classified as coarse or colloid, according to their size. Clay, silt, micro-organisms, organic matter, effluent discharge are the main sources of colloidal particles. Suspended particles and colloids prevent the passage of light through the water [6]. Besides compromising the quality of the water body, the turbidity leads to the increasing of costs in the treatment of the water, mainly in the process of chemical coagulation, and also in the increasing of sludge production [1].

Some cyanobacteria are also related to the odor, flavor, and release of toxins into the water. Thus, waters containing cyanobacteria need special attention since they lead to preoccupations regarding the quality of the waters and public health [7].

The conventional treatment system usually begins in the coagulation process, followed by other processes to separate solids from liquids, as flocculation, sedimentation or flotation, and the filtration. The goal is that the removal of the algae takes place without damaging its cells, and consequently without the liberation of its toxins [7]. The conventional treatment shows not to be sufficient at some specific scenarios, bringing the necessity of the application of new technologies to complement it [1].

The presence of phytoplanktonic organisms in the waters destined to WTP's require a higher quantity of chemical products for an efficient coagulation, several times being necessary the use of polymers to help the sedimentations of the flocs. Such process increases the mass of waste, in addition to clogging the filter media, this results in more water for washing and lower disinfection and water production efficiency [8].

In this context, the use of mathematical models by the colloidal theory helps the qualitative and quantitative comprehension of the nature of the interaction between the colloids and the forces acting upon them. It can guide the steps in the process of coagulation and lead to its optimization. Such characteristics turn the mathematical modelling a sustainability tool by giving aids for the understanding of the physical behavior of colloidal complexes in the raw water and of those formed after filtration. Contributing, thus, to a more efficient and sustainable treatment, since it implies in the economy of financial resources, smaller quantity of chemical products and the consequent moderation in the use of natural resources.

Several authors have studied the interaction of biocolloids with sand or clay particles, aiming at their removal. The study of interaction forces allowed MS2 and ΦX174 bacteriographs to be used as model viruses by [9, 10] to study their interaction with clay particles. Bacterial fixation on clay particles has become increasingly important, such as the studies on the fixation of *Pseudomonas (P.)* [11, 12] on kaolinite, where the best fixation occurred on poorly crystallized kaolinite [11]. The studies also cover the evaluation of the distribution of fecal viral indicators between kaolinite and bentonite [13]; virus transport in groundwater and its fixation in quartz sand [14]; between others.

With this in mind, the goal of the present work is to apply the mathematical modelling by the colloidal theory in the double filtration: gravel upflow filtration followed by sand downflow rapid filtration. The study water contains cyanobacteria (*Microcystis* spp.) in order to express the interaction between the biocolloids in the situations before and after the chemical coagulation and during and after the filtration, by means of the colloidal XDLVO theory (Extended Derjarguin-Landau-Verwey-Overbeek).

MATERIAL AND METHODS

This work is divided into two main steps: the acquisition of experimental data and the application of the mathematical model. For the application of the mathematical modelling by means of the XDLVO theory, it will be necessary data of the characteristics of the study water (SW), coagulated water (CW) and the porous media, such data was obtained from [15] and [16].

The mathematical equations to be used refer to the attractive and repulsive forces under which the biocolloidal particles are subjected. The modelling of the equations and their applications were conceived in electronic worksheets of Excel® pertaining to the package Microsoft Office®.

Acquisition of experimental data

The experimental data obtained from [15] regard the characteristics of the study water (SW), coagulated water (CW), gravel upflow filtration (GUF) and sand downflow rapid filtration (SDRF).

Among the five essays (ESY 1- ESY 5) with the study water-2 (SW-2) realized in [15], ESSAY 2 was selected for the application of the model. The scheme of the step of the treatment are presented in Figure 1.

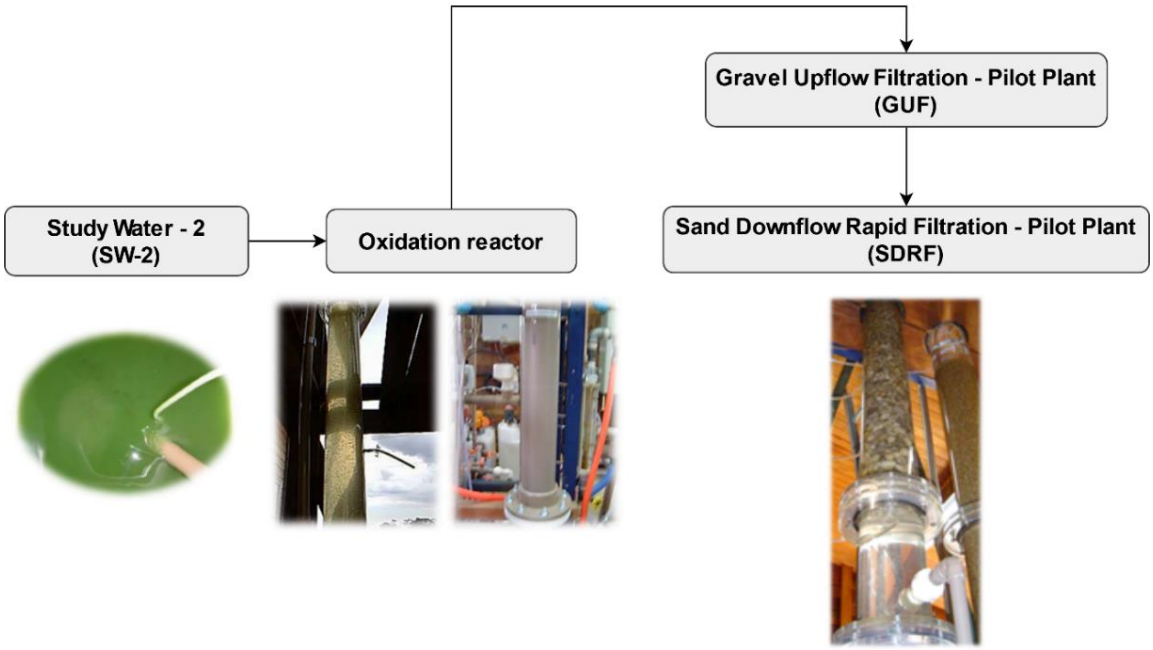

Figure 1. Experimental Pilot Plant Treatment system used in the tests to evaluate the removal of cells and by-products of *Microcystis* spp. Adapted from [15].

The SW consists of water with addition of compounds or micro-organisms in a specific concentration for the desired use in tests of treatability and experiments in pilot plant installation. In the case if the cited work, the SW was prepared with addition of culture of *Microcystis* spp. with densities close to 10^5 cells.mL^{-1}, and total microcystins (MC) concentrations between 10 µg.L^{-1} and 20 µg.L^{-1}, named SW-2, consisting of filtered water without chlorination from the well water (ETASC2) with addition of culture of cyanobacteria and extract of MC's not purified (PHASE 2). After its preparation, the SW went through the oxidation reactor with addition of chlorine, followed by the coagulation process with aluminum sulfate and finally with the double filtration system [15].

The relevant characteristics of the study water of the aforementioned ESY 2 are shown in Table 1.

Table 1. Characterization of the study water used in Essay 2. Adapted from [15].

Parameters	Essay 2
pH	6.64
Apparent color (uH)	24
True color (uH)	2.0
Turbidity (uT)	2.36
Total alkalinity (mg $CaCO_3$/L)	6.0
Total hardness (mg $CaCO_3$/L)	20
Acidity	3.0

With respect to the porous media, the granular materials used in the GUF and SDRF have the average grain sizes of 13.4 mm and 0.85 mm, and zeta potential varying from -2.5 to -1.2 mV and from -2.1 to -1.8, respectively.

Finally, the Table 2 shows the results of temperature (ºC), hydrogen potential (pH) and zeta potential (ZP (mV)), obtained in ESY 2 and the efficiency in the reduction of the density of *Microcystis* spp. in GUF and SDRF, which will be used in the mathematical model of the colloidal theory (XDLVO).

Table 2. Control parameters for ESY 2. Adapted from [15].

Hour (h)	**T (ºC)**	**pH**	**ZP (mV) SW**	**pH**	**ZP (mV) CW**	**pH**	**ZP (mV) GUF**	**pH**	**ZP (mV)** SDRF
1	22.50	7.02	-28.8	6.92	-26.6	6.74	-2.00	6.68	-1.80
3	21.75*	7.09*	-34.6	6.97	-24.0	6.88	-1.20	6.90*	-2.00
6	21.75*	7.24	-26.1	6.96	-25.2	6.86	-2.50	6.88	-2.10
7	21.00	7.09	-31.3	6.96	-21.4	6.86	-1.92*	6.90*	-1.98*
10	21.75*	7.01	-24.9	6.96	-21.7	7.09	-2.00	7.13	-2.00
Partial Efficiency			-		-		46.2%		0.3%
Total Efficiency			-		-		99.7%		99.9%

*Average value due to the absence of data in [15].

Application of the mathematical modelling

Understanding the stabilization of the colloids gives information about it aggregation dynamics [17]. The equilibrium between the acting forces considered by the XDLVO theory (Extended Derjarguin-Landau-Verwey-Overbeek), also known as intermolecular forces, control the stability of the particles in the colloidal system [18].

The use of the XDLVO theory, and not the DLVO theory (previous version), is justified because its extended version includes factors not accounted for previously, such as, for example, the Lewis acid-base force, which is important in the analysis of the behavior of barriers of energy [9], as well as, it was fundamental in the studies where this theory has been widely in various situations, as in the petroleum industry to understand the interaction between particles under different salinities and rocks [19], studies to comprehend how such factors influence the transport of thin particles in porous media [20], research on the influence of the pH value in the encrustation of membranes [21], investigation of the modifications in the plasma surface aiming to decrease the adsorption of nano and micro-plastics [22], joint application of the modified Poisson-Boltzmann equation to quantify the interaction energy between fouling and charged membrane [23], joint evaluation with thermodynamic analysis and DLVO (Derjaguin-Landau-Verwey-Overbeek) theory to study the adhesion of bacteria on montmorillonite [24].

The XDLVO theory defines the total energy or total interaction force of a system, taking into account both attractive and repulsive forces [19]. The forces considered in this work include the acid-base interaction (AB), Lifshitz-Vander Waals (vdW), double electric layer (DEL) and Born repulsion forces.

The Lewis acid-base force is a short range interaction at the solid-liquid interface. It can be attract or repel, and is represented by the transfer of a pair of electrons from a base to an acid [25].

The Lifshitz-Vander Waals force is an attractive force between two particles, where temporary dipoles in a particle induce dipoles in another particle. It depends on the geometry and also on the macroscopic electromagnetic features of the interacting bodies, giving rise to the Hamaker's constant [26], an intrinsic coefficient related to the inter-particle energy, and whose values usually varies from 10^{-21} to 10^{-19} J [19].

The double electric layer force occurs when the particles are negatively charged and attract positive ions of the solution, i.e., the double layer is formed under a charged surface immersed in a fluid. The first layer is called "Stern's layer or compact layer" formed by counter-ions, and the second is called "diffuse layer", formed by ions [20]. The potential difference between these two layers is the zeta potential (φ), and it is used to compute the energy of the interaction of the double electric layer. Another parameter present is the Debye length (K), which indicates the thickness of the double electric layer [19].

Finally, the Born repulsion force arises when particles are close and the electron clouds superimpose, being therefore of short range [27]. It is heavily influenced by the structures of the surfaces in contact with the liquid. It occurs only when the particles are very close to each other, since when the distance is greater than 1 nm, the Born force does not contribute to the total energy of total force of the system [19]. The Hamaker constant and the atomic collision diameter are extremely important for the computation of this force.

The diameter of the particle (d_p) is usually much smaller than the diameter of the collector (d_c), and one considers the particle as a sphere and the surface of the collector a plane [28]. The geometric combinations to be used are shown in Figure 2. The main goal is to compute the free energy and force of interaction ($\Delta G_{Total}{}^{XDLVO}$ and $\Delta F_{Total}{}^{XDLVO}$) as a function of the separation distance between the particles (δ).

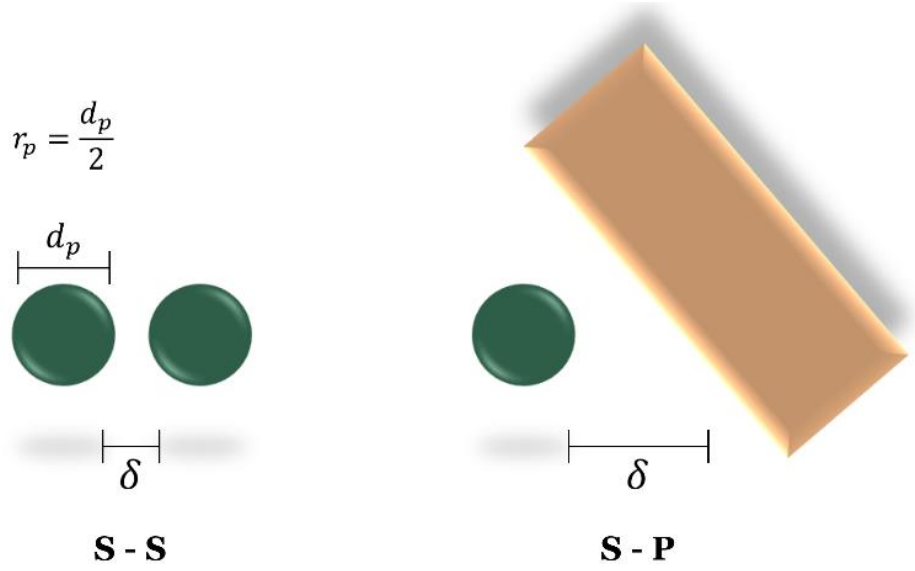

Figure 2. Arrangements of interaction between surfaces, geometries, and dimensions for mathematical modeling by colloidal theory: (S-S) refers to the interaction between spheres (*Microcystis spp*.) and (S-P) refers to the interaction between spherical particle and plane collector (*Microcystis* spp. and grain of sand or gravel).

The equations for the intermolecular forces are presented in Table 3. The superscripts of the equations refer to: " DEL - force or energy of the double electric layer; "AB" - Lewis AB force or energy; "vdW" - Lifschitz - Vander Waals force or energy; "Born" - Born repulsive force or energy; “pwc” – particle-water-collector; and “pw” – particle-water.

Table 3. XDLVO theory intermolecular force equations.

Equation	References
$* \Delta G^{DEL} = \pi . \varepsilon_a . r_p . \left[2\varphi_{\mathrm{p}} \varphi_{\mathrm{c}} . ln\left(\frac{1+\exp(-K\delta)}{1-\exp(-K\delta)}\right) + \left(\varphi_{\mathrm{p}}{}^2 + \varphi_{\mathrm{c}}{}^2\right) . \ln(1-\exp(-2K\delta)) \right]$	[29]
$* \Delta F^{DEL} = 64\pi . \varepsilon_a . \mathrm{K} . r_p . \left(\frac{k_B . T}{Z . e}\right)^2 . tanh\left(\frac{Z . e . \varphi_{\mathrm{p}}}{4 k_B . T}\right) . tanh\left(\frac{Z . e . \varphi_{\mathrm{c}}}{4 k_B . T}\right) . \exp(-\mathrm{K} . \delta)$	[26]
$** \Delta G^{DEL} = 2\pi . \varepsilon_a . r_p . \varphi_p{}^2 \left[ln\left(\frac{1+\exp(-K\delta)}{1-\exp(-K\delta)}\right) + \ln(1-\exp(-2K\delta)) \right]$	[21]
$** \Delta F^{DEL} = 32\pi . \varepsilon_a . \mathrm{K} . r_p . \left(\frac{k_B . T}{Z . e}\right)^2 . tanh\left(\frac{Z . e . \varphi_{\mathrm{p}}}{4 k_B . T}\right)^2 . \exp(-\mathrm{K} . \delta)$	[30]
$\mathrm{K} = \sqrt{\frac{2F^2 . I . 10^3}{\varepsilon_a . R . T}}$	[26]
$* \Delta G^{AB} = 2\pi . r_p . \lambda_{AB} . \Delta G_{\delta_0}{}^{AB} . \exp\left(\frac{\delta_0 - \delta}{\lambda_{AB}}\right)$	[21, 25, 30, 31]
$* \Delta F^{AB} = 2\pi . r_p . \Delta G_{\delta_0}{}^{AB} . \exp\left(\frac{\delta_0 - \delta}{\lambda_{AB}}\right)$	[28]
$** \Delta G^{AB} = \pi . r_p . \lambda_{AB} . \Delta G^{AB} . \exp\left(\frac{\delta_0 - \delta}{\lambda_{AB}}\right)$	[28]
$** \Delta F^{AB} = \pi . r_p . \Delta G^{AB} . \exp\left(\frac{\delta_0 - \delta}{\lambda_{AB}}\right)$	[28]
$\Delta G_{\delta_0,pwc}{}^{AB} = 2 . \left[\sqrt{\gamma_3^+} . \left(\sqrt{\gamma_1^-} + \sqrt{\gamma_2^-} - \sqrt{\gamma_3^-}\right) + \sqrt{\gamma_3^-} . \left(\sqrt{\gamma_1^+} + \sqrt{\gamma_2^+} - \sqrt{\gamma_3^+}\right) - \sqrt{\gamma_1^+ . \gamma_2^-} - \sqrt{\gamma_1^- . \gamma_2^+} \right]$	[32]

Cont. Table 3

$\Delta G_{\delta_0,pw}{}^{AB} = -4.\left(\sqrt{\gamma_2^+} - \sqrt{\gamma_3^+}\right).\left(\sqrt{\gamma_2^-} - \sqrt{\gamma_3^-}\right)$	[33]
$*\ \Delta G^{vdW} = \frac{H.r_p}{6\delta}.\left[1 - \frac{5{,}32\delta}{\lambda_w}.ln\left(1 + \frac{\lambda_w}{5{,}32\delta}\right)\right]$	[20]
$*\ \Delta F^{vdW} = \frac{H.r_p}{6\delta^2}.\left(\frac{5{,}32\delta}{\lambda_w} + 1\right)^{-1}$	[20]
$**\ \Delta G^{vdW} = \frac{H.r_p}{12\delta}.\left[1 - \frac{5{,}32\delta}{\lambda_w}.ln\left(1 + \frac{\lambda_w}{5{,}32\delta}\right)\right]$	[28]
$**\ \Delta F^{vdW} = \frac{H.r_p}{12\delta^2}.\left(\frac{5{,}32\delta}{\lambda_w} + 1\right)^{-1}$	[28]
$H_{pwc} = \left(H_{12}{}^{1/2} - H_{33}{}^{1/2}\right).\left(H_{22}{}^{1/2} - H_{33}{}^{1/2}\right)$	[34]
$H_{pw} = \left(H_{12}{}^{1/2} - H_{33}{}^{1/2}\right)^2$	[26]
$*\ \Delta G^{Born} = -\frac{H.x^6}{7560}.\left[\frac{8r_p + \delta}{\left(2r_p + \delta\right)^7} + \frac{6r_p - \delta}{\delta^7}\right]$	[35, 36, 37]
$*\ \Delta F^{Born} = -\frac{H.x^6.r_p}{180\delta^8}$	[38]
$**\ \Delta G^{Born} = -\frac{H.x^6.r_p}{1260.\delta^7}$	[26]
$**\ \Delta F^{Born} = -\frac{H.x^6.r_p}{180.\delta^8}$	[20]

*Equations for sphere-plane interaction; **Equations for interaction for sphere-sphere.

Some constants values of the equations will be obtained from the literature, as the Hamaker constant, which varies for each type of material: collector (sand or gravel), particle (*Microcystis* spp. in aqueous media), and water; the values of the superficial tensions; the Born collision and repulsion diameters; wave length decay and the Lewis AB approximation distance, among others. The Table 4 shows the definition of each parameter, values and their units.

Table 4. Parameters used in XDLVO theory.

Parameters	Definition	Values [Units]	References
k_B	Boltzmann constant	$1.3808.10^{-23}$ J.K^{-1}	[39, 40]
e	Electron charge	$1.602.10^{-19}$ C	[39]
ε_a	Permissiveness coefficient of the solution	$6.9539.10^{-10}$ C^2/Jm	[39, 40]
R	Avogadro's constant	$6.02.10^{23}$ mol^{-1}	[39]
F	Faraday's constant	96485 C/mol	
r_p	Particle radius	0.000002 m	[39, 41]
φ_p/φ_c	Particle/Collector zeta potential *	V	[15]
H	Hamaker's constant*	J	[28, 42]
γ^+/γ^-	Recipient/Donor surface tension*	mJ/m^2	[28, 43]
T	Temperature*	K	[15]
Z	Valence of the ion	1 (admensional)	
λ_w	Wavelength of light scattered between particles	100 nm	[44]
K	Debye-Huckel constant*	m^{-1}	[25]
X	Collision diameter	0.5 nm	
λ_{AB}	Wavelength of scattered light for acid-base interaction	0.6 nm	
δ	Separation distance	nm	
δ_0	Minimum separation distance	0.16 nm	[45]
I	Ionic strength of the system	0.0212 mol/L	[4]

*Variable parameters.

RESULTS AND DISCUSSION

The arrangements of interaction and geometry adopted in this work correspond to the sphere-sphere (S-S) for the study water (SW) and coagulated water (CW); the sphere-sphere and the sphere-plane (S-P) for the double filtration system (gravel upflow filtration (GUF) and sand downflow rapid filtration (SDRF)).

The legend admits the configuration in which the cyanobacteria particle are represented by the sphere and the collectors (gravel and sand) being represented by the plane. The symbols "ΔG" and "ΔF" represent the energy and force variation, respectively.

Due to the absence of data in the literature, the Hamaker constant and the values of the superficial tensions for the gravel material are the same as the ones used for sand, obtained from [25].

By means of the application of the XDLVO theory, results were obtained after modelling in electronic worksheets in Microsoft Excel®, represented later as graphs.

Figure 3 presents the model applied to the study water, composed of water and cyanobacteria *Microcystis* spp. One has thus just the modelling for the combination sphere-sphere (particle-particle).

In the graphics (a) and (b) one observes that the Born and vdW energies and forces have great influence at short distances. The DEL and AB energies for the graphic (a), on the other hand, manifest at longer distances. In the graphic (b), the vdW force is small and the AB begins at 300 nN and remains for longer distances compare to the other forces. The XDLVO energy reached its maximum at 0.16 nm with 224854.78 kT.

Observing the total energy of the system it is possible to notice that it can vary from negative to positive, depending on the summation of the intermolecular forces involved, as seen in the transition of the graphic (c) from 0.1 nm.

Starting from the analysis of the coagulated water, one has the results presented in Figure 4.

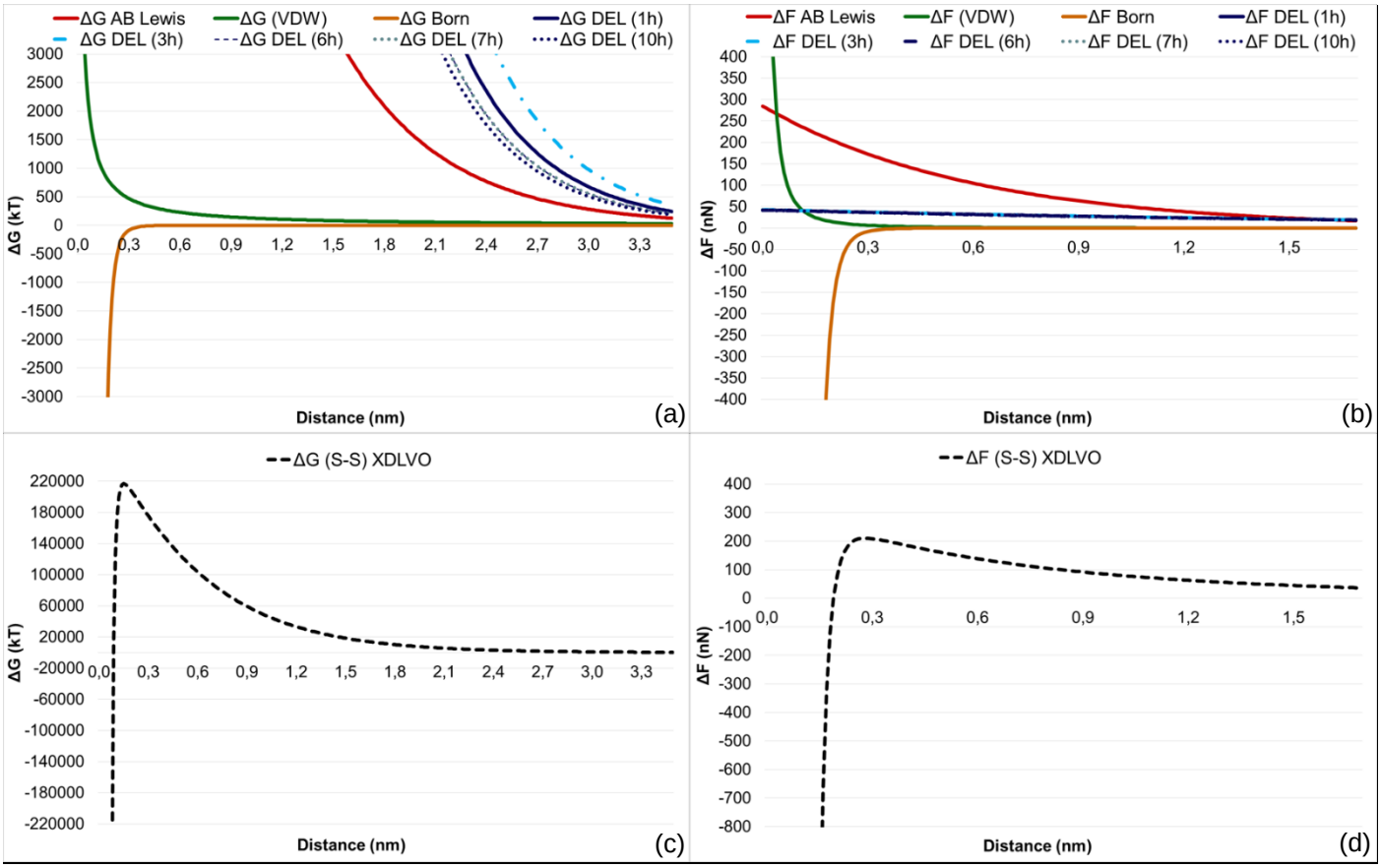

Figure 3. Behavior of intermolecular forces over distance for study water. (a) Individual energies for sphere-sphere interaction. (b) Individual forces for sphere-sphere interaction. (c) Total energy in sphere-sphere interaction. (d) Total force in sphere-sphere interaction.

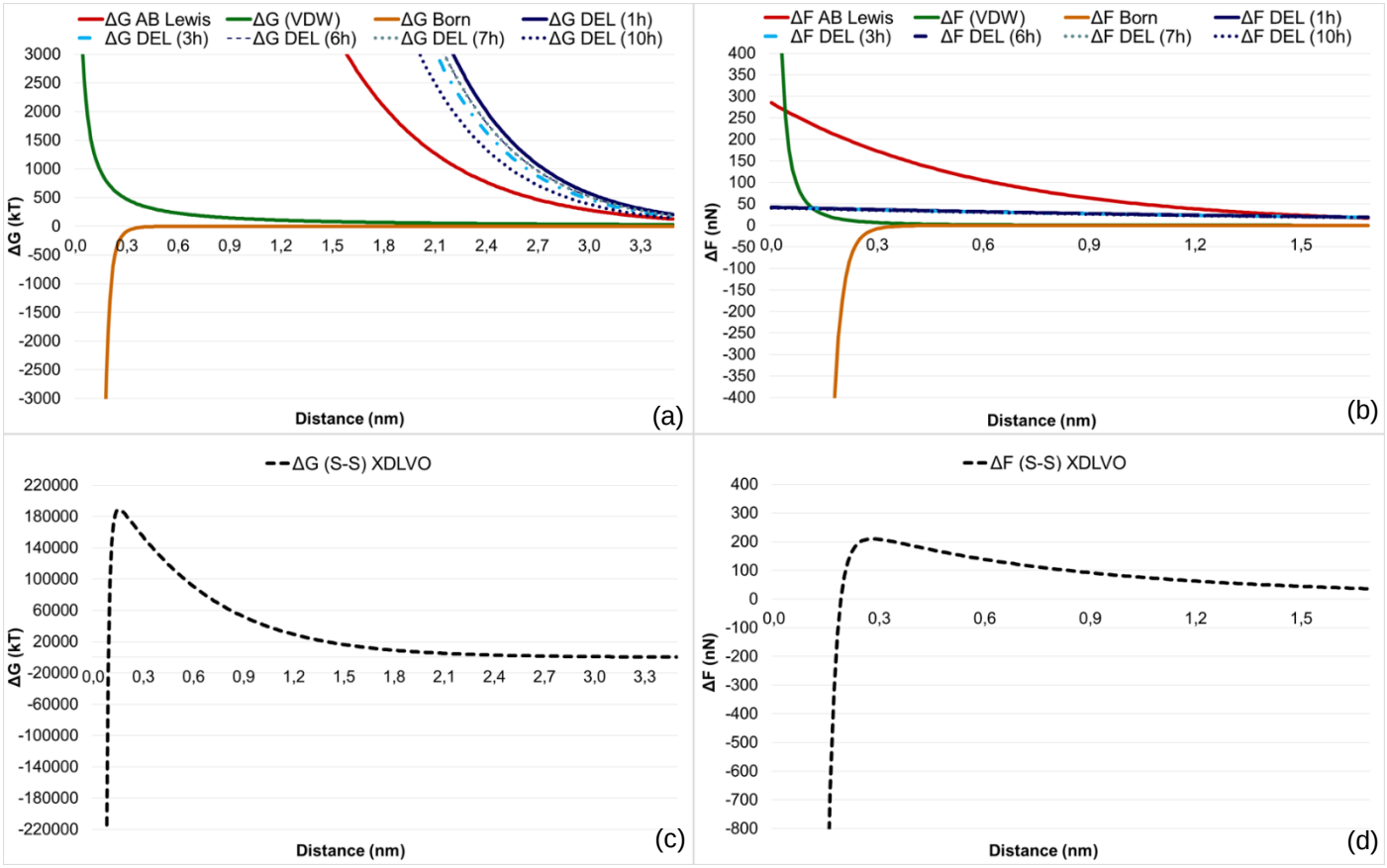

Figure 4. Behavior of intermolecular forces over distance for coagulated water. (a) Individual energies for sphere-sphere interaction. (b) Individual forces for sphere-sphere interaction. (c) Total energy in sphere-sphere interaction. (d) Total force in sphere-sphere interaction.

The only varied parameter in this phase was the zeta potential of the cyanobacteria *Microcystis* spp., and as a consequence the only modified force was the double electric layer. Here, the coagulated water showed a pattern similar to the study water, with a certain decrease in the DEL energy, for as presented in Table 2, the zeta potential decreases in absolute value along the treatment until the step of double filtration, leading in a lower total energy balance.

This reduction of the absolute value of the zeta potential is due to the action of aluminum sulfate coagulant, resulting now in a destabilized system and in the decrease of the total energy (XDLVO), since this chemical agent acts in the compression of the double layer and in the respective reduction of the repulsion barrier in the colloidal theory, as it is evident when comparing Figures 3(c) and 4(c).

The total XLDVO energy reached its maximum at 0.17 nm with 15352.03 kT, with difference of 67505.75 kT when compared to the water without coagulant.

Comparing the graphics of force, one sees that the variations was of the order of 8.88 nN.

Figure 5 makes evident the XDLVO theory applied to the gravel upflow filtration. From this step of the treatment it was used the modelling for the sphere-plane combination (particle-collector).

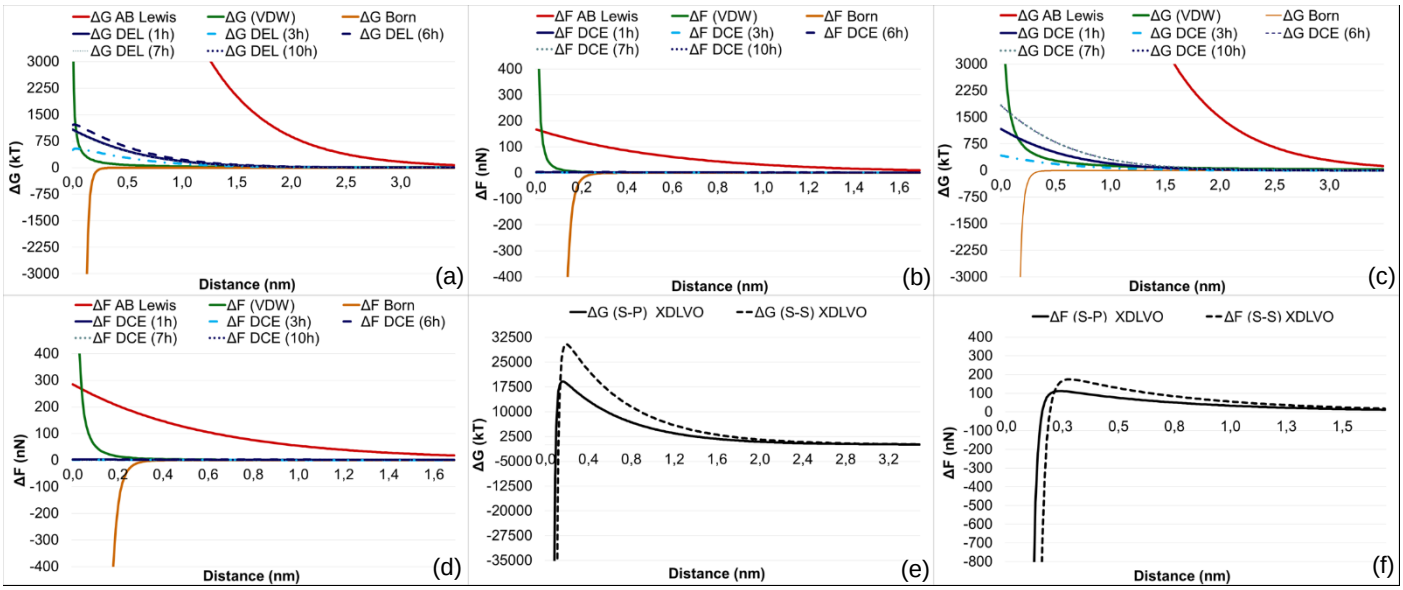

Figure 5. Behavior of intermolecular forces over distance for gravel upflow filtration. (a) Individual energies for sphere-plane interaction. (b) Individual forces for sphere-plane interaction. (c) Individual energies for sphere-sphere interaction. (d) Individual forces for sphere-sphere interaction. (e) Total energy in sphere-plane/sphere-sphere interaction. (f) Total force in sphere-plane/sphere-sphere interaction.

Analyzing the interaction sphere-sphere and comparing CW with GUF, the differences are more evident at DEL, because the reduction in absolute value of the zeta potential was drastic, decreasing heavily the DEL energy, and the force became practically null, increasing the attraction potentials.

The reduction is even more drastic when evaluating ΔG_{Total}^{XDLVO}, having its maximum at 0.2 nm with 30359.15 kT, leading to a reduction of 126992.88 kT when compared to the coagulated water.

When regarding the interaction sphere-plane the difference are more substantial at DEL, even though the other forces were also modified. Note that the ΔG_{Total}^{XDLVO} has a lower maximum energy (19138.79 kT) when the geometries have this configuration.

All graphics showed that the force manifest at shorter distances, while in terms of energy the contrary happens.

Figure 6 shows the XDLVO theory applied to the sand downflow rapid filtration.

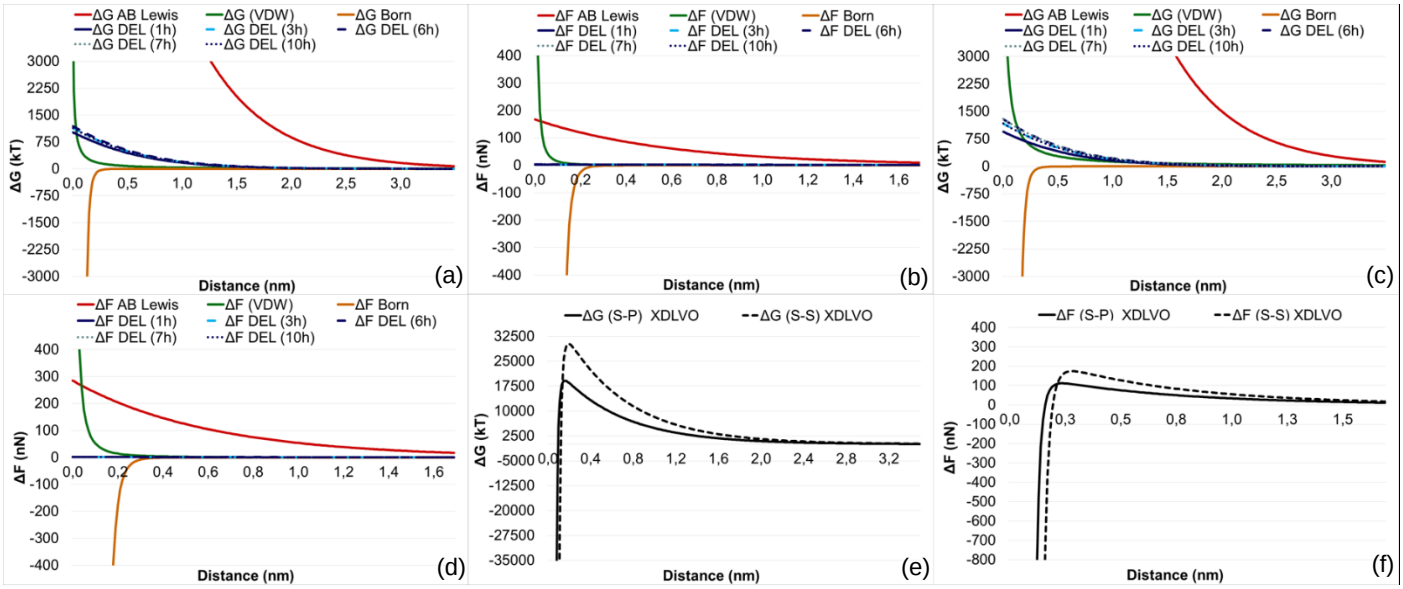

Figure 6. Behavior of intermolecular forces over distance for sand downflow rapid filtration. (a) Individual energies for sphere-plane interaction. (b) Individual forces for sphere-plane interaction. (c) Individual energies for sphere-sphere interaction. (d) Individual forces for sphere-sphere interaction. (e) Total energy in sphere-plane/sphere-sphere interaction. (f) Total force in sphere-plane/sphere-sphere interaction.

As the variations of the zeta potential between the steps of GUF and SDRF were low, consequently, the variations in the values of energy and force had small variations. This can be better observed in Table 5, which shows the maximum and minimum values of $\Delta G_{Total}{}^{XDLVO}$ and $\Delta F_{Total}{}^{XDLVO}$, analyzed at a separation distance among 0.01 to 5 nm.

Table 5. Table of maximums and minimums for $\Delta G_{Total}{}^{XDLVO}$ and $\Delta F_{Total}{}^{XDLVO}$.

TREATMENT PHASES	MAXIMUMS		MINIMUMS	
	Value (kT) Distance (nm)	*Value (nN) Distance (nm)*	*Value (kT) Distance (nm)*	*Value (nN) Distance (nm)*
SW (S-S)	224854.78	210.00	$-2.33.10^{12}$	$-6.65.10^{12}$
	0.16	0.29	0.01	0.01
CW (S-S)	157352.03	209.12	$-2.33.10^{12}$	$-6.65.10^{12}$
	0.17	0.29	0.01	0.01
GUF (S-S)	30359.15	174.22	$-2.33.10^{12}$	$-6.65.10^{12}$
	0.20	0.29	0.01	0.01
GUF (S-P)	19138.79	111.47	$-3.26.10^{11}$	$-9.29.10^{11}$
	0.17	0.25	0.01	0.01
SDRF (S-S)	30367.70	174.24	$-2.33.10^{12}$	$-6.65.10^{12}$
	0.20	0.29	0.01	0.01
SDRF (S-P)	19218.23	111.68	$-3.26.10^{11}$	$-9.29.10^{11}$
	0.17	0.25	0.01	0.01

Figure 7 exhibits the comparison of the variation of energy (a) and force (b) of interaction, respectively, as a function of the separation distance, by the colloidal theory between the beginning and the end of the treatment, i.e., between the study water after the sand downflow rapid filtration.

One notice that the treatment applied to the study water showed positive effects in the reduction of the absolute value in the energy barrier (repulsion energy), and therefore of the repulsion forces in the XDLVO theory, making the particles (*Microcystis* spp.) available to removal by treatment. The graphics (a) and (b), approximately at 0.16 and 0.25 nm, respectively, make it evident in which distance occurred the maximum peak of colloidal electrostatic destabilization of the particles *Microcystis* spp.

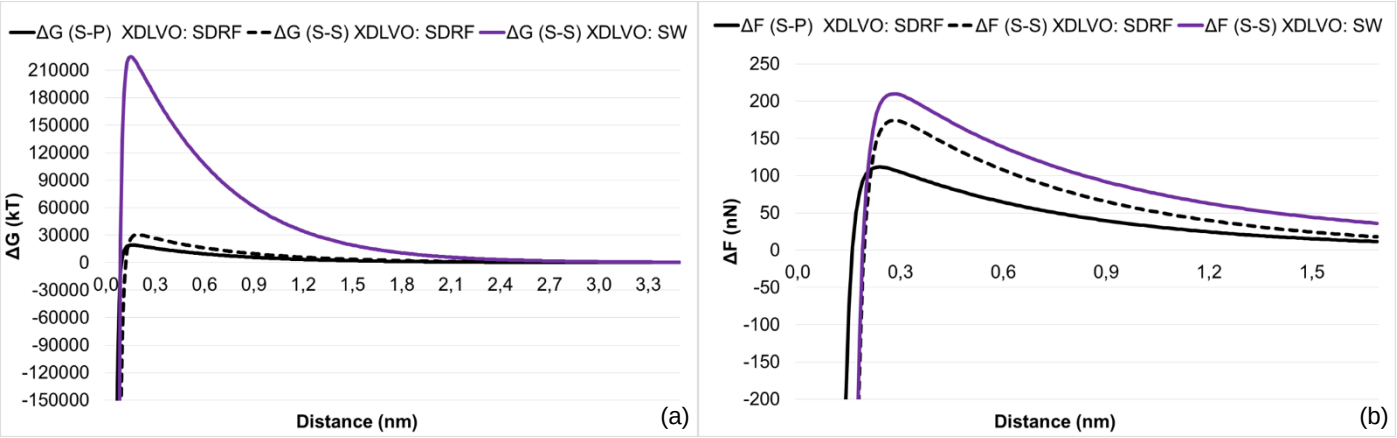

Figure 7. Comparison of the variation of results between SW and after SDRF. (a) Total energy graph. (b) Total force graph.

CONCLUSION

This work allowed to evaluate the efficiency of some steps of the treatment for the removal of cyanobacteria *Microcystis* spp. by the system of treatment by double filtration.

The action of the coagulant in the XDLVO theory altered the behavior of the forces of interaction, principally in regards to the decreasing of the absolute value of the electric potential of the double layer which encloses the colloidal particles. This initial destabilization allowed the zeta potential to decrease more expressively in the step of double filtration, allowing an instability scenario.

The standard configuration of $\Delta G_{Total}{}^{XDLVO}$ and $\Delta F_{Total}{}^{XDLVO}$ were similar, both decreasing along the steps of treatment. The energy, though, showed larger absolute values.

The XDLVO theory was capable of evaluate the treatment of waters with respect to the removal of cyanobacteria, making it explicit the reduction of energy and forces which integrate the colloidal systems along the separation distance, making viable the removal of these particles after their microscopic destabilization. Evaluating the results of the study water and filtered water, it was possible to describe the behavior of the biocolloids along the treatment by double filtration.

It was verified, therefore, that the *Microcystis* spp. particles became unstable due to the double filtration, since the repulsion energetic barrier of the raw water decreased approximately 90% such repulsion.

The present study may contribute to the understanding of the interaction and removal of biocolloids such *Microcystis spp.* with porous media type sand and gravel particles in double filtration process, as well as to estimate the efficiency of the desired treatment in waters containing Microcystis spp. In addition, this study contributes to a moderation in the use of natural resources (sustainability) as it can enable to improvement the double filtration process in the design of drinking water plants.

Funding: This research received no external funding.
Conflicts of Interest: The authors declare no conflict of interest.

REFERENCES

1. Glusczak AG, Graepin C, Somavilla EA, Carissimi E. Remoção de turbidez para pré-tratamento de água por eletrocoagulação. In: Anais do 11º Simpósio Internacional de Qualidade Ambiental; 2018 Out 02-04; Porto Alegre, Brasil.
2. Lin L, Zhang Y, Yan W, Fan B, Fu Q, Li S. Performance of gravity-driven membrane systems for algal water treatment: Effects of temperature and membrane properties. Sci Total Environ. 2022; 838(155963):1-12.
3. Zhu T, Zhou Z, Qu F, Liu B, Bruggen BV. Separation performance of ultrafiltration during the treatment of algae-laden water in the presence of na anionic surfactant. Sep Purif Technol. 2022;281(119894):1-10.
4. Zhang B, Tang H, Huang D, Gao X, Zhang B, Shen Y, et al. Effect of pH on anionic polyacrylamide adhesion: New insights into membrane fouling based on XDLVO analysis. J Mol Liq. 2020;320(114463):1-9.
5. Liu B, Qu F, Liang H, Gan Z, Yu H, Li G, et al. Algae-laden water treatment using ultrafiltration: Individual and combined fouling effects of cells, debris, extracelular and intracelular organic matter. J Memb Sci. 2017;528:178-86.
6. Di Bernardo AS. Desempenho de sistemas de dupla filtração no tratamento de água com turbidez elevada [doctoral thesis]. São Carlos: Escola de Engenharia de São Paulo, Universidade de São Paulo; 2004. 301 p.
7. Ren B, Weitzel KA, Duan X, Nadagouda MN, Dionysiou DD. A comprehensive review on algae removal and control by coagulation-based processes: mechanism, material, and application. Sep Purif Technol. 2022;293(121106):1-26.
8. De Pádua VL, Di Bernardo L. Método comparativo do tamanho dos flocos formados após coagulação com sulfato de alumínio e cloreto férrico. In: Anais do Congreso Interamericano de Ingeniería Sanitaria y Ambiental. 2000; Porto Alegre, RS.
9. Chrysikopoulos CV, Syngouna VI. Attachment of bacteriophages MS2 and X174 onto kaolinite and montmorillonite: Extended-DLVO interactions. Colloids Surf B Biointerfaces. 2012;92:74-83.
10. Syngouna VI, Chrysikopoulos CV. Interaction between Viruses and Clays in Static and Dynamic Batch Systems. Environ. Sci. Technol. 2010;44:4539-4544.
11. Vasiliadou IA, Papoulis D, Chrysikopoulos CV, Panagiotaras D, Karakosta E, Fardis M, Papavassiliou G. Attachment of Pseudomonas putida onto differently structured kaolinite minerals: A combined ATR-FTIR and 1H NMR study. Colloids Surf B Biointerfaces. 2011;84:354-359.
12. Chrysikopoulos CV, Syngouna VI, Vasiliadou IA, Katzourakis VE. Transport of *Pseudomonas putida* in a 3-D Bench Scale Experimental Aquifer. Transp Porous Med. 2012;94:617-642.
13. Bellou MI, Syngouna VI, Tselepi MA, Kokkinos PA, Paparrodopoulos SC, Apostolos V, et al. Interaction of human adenoviruses and coliphages with kaolinite and bentonite. Sci Total Environ. 2015;517:86-95.
14. Chrysikopoulos CV, Aravantinou AF. Virus attachment onto quartz sand: Role of grain size and temperature. J. Environ. Chem. Eng. 2014;2:796-801.

15. Kuroda EK. Remoção de células e subprodutos de Microcystis spp. por dupla filtração, oxidação e adsorção [doctoral thesis]. São Carlos: Escola de Engenharia de São Paulo, Universidade de São Paulo; 2006. 267 p.
16. Kuroda EK. Avaliação da filtração direta ascendente em pedregulho como pré-tratamento em sistemas de dupla filtração [master's thesis]. São Carlos: Escola de Engenharia de São Paulo, Universidade de São Paulo; 2002. 242 p.
17. Lu D, Fatehi P. Interfacial interactions of rough spherical surfaces with random topographies. Colloids Surf A Physicochem Eng Asp. 2022;642(128570):1-13.
18. Carstens JF, Bachmann J, Neuweiler I. A new approach to determine the relative importance of DLVO and non-DLVO colloid retention mechanisms in porous media. Colloids Surf A. 2019;560:330-5.
19. Muneer R, Hashmet MR, Pourafshary P. Predicting the critical salt concentrations of monovalente and divalent brines to initiate fines migration using DLVO modeling. J Mol Liq. 2022;352(118690):1-12.
20. Yang Y, Yuan W, Hou J, You Z. Review on physical and chemical factors affecting fines migration in porous media. Water Res. 2022;214(118172):1-16.
21. Zhang T, Zhan J, Wang Q, Zhang H, Wang Z, Wu Z. Evaluating of the performance of natural mineral vermiculite modified PVDF membrane for oil/water separation by membrane fouling model and XDLVO theory. J Memb Sci. 2022;641(119886):1-12.
22. Enfrim M, Wang J, Merenda A, Dumée LF, Lee J. Mitigation of membrane fouling by nano/microplastics via surfasse chemistry control. J Memb Sci. 2021;633(119379):1-9.
23. Jiang L, Chen L, Zhu L. In-situ electric-enhanced membrane distillation for simultaneous flux-increasing and anti-wetting. J Memb Sci. 2021;630(119305):1-12.
24. Ruan B, Wu P, Liu J, Jiang L, Wang H, Qiao J, et al. Adhesion of *Sphingomonas* sp. GY2B onto montmorillonite: A combination study by thermodynamics and the extended DLVO theory. Colloids Surf B Biointerfaces. 2020;192(111085):1-10.
25. Fan Z, Ji P, Zhang J, Segets D, Chen D, Chen S. Wavelet neural network modeling for the retention efficiency of sub-15 nm nanoparticles in ultrafiltration under small particle top ore diameter ratio. J Memb Sci. 2021;635(119503):1-11.
26. Nikoo AH, Kalantariasl A, Malayeri MR. Propensity of gypsum precipitation using surfasse energy approach. J Mol Liq. 2020;300(112320):1-15.
27. Yue L, Pu W, Zhao S, Zhang S, Ren F, Xu D. Insights into mechanism of low salinity water flooding in sandstone reservoir from interfacial features of oil/brine/rock via intermolecular forces. J Mol Liq. 2020;313(113435):1-14.
28. Botari A, Di Bernardo L, Dantas AD. Análise de modelação matemática da interação entre partículas na filtração direta utilizando a teoria coloidal. Eng Sanit Ambient. 2012;17(1):81-94.
29. Wu H, Shen F, Wang J, Wan Y. Membrane fouling in vacum membrane distillation for ionic liquid recycling: Interation energy analysis with the XDLVO approach. J Memb Sci. 2018;550:436-47.
30. Ou Q, Xu Y, Li X, He Q, Liu C, Zhou X, et al. Interactions between activated sludge extracelular polymeric substances and model carrier surfaces in WWTPs: A combination of QCM-D, AFM and XDLVO prediction. Chemosphere. 2020;253(126720):1-10.
31. Zou W, Zhao J, Sun C. Adsorption of Anionic Polyacrylamide onto Coal and Kaolinite Calculated from the Extended DLVO Theory Using the van Oss-Chaudhury-Good Theory. J Polym. 2018;10(113):1-11.
32. Flores AG, Solong SK, Heyes GW, Ilyas S, Kim H. Bubble-particle interactions with hydrodynamics, XDLVO theory, and surfasse roughness for flotation in na agitated tank using CFD simulations. Miner Eng. 2020;152(106368):1-11.
33. Yang L, Wen J. Can DLVO theory be applied to MOF in diferente dieletric solventes? Microporous and Mesoporous Materials. Microporous Mesoporous Mater. 2022;343(112166):1-9.
34. Xie Q, Saeedi A, Piane CD, Esteban L, Brady PV. Fines migration during CO_2 injection: Experimental results interpreted using surfasse forces. Int. J. Greenh. Gas Control. 2018;65:32-9.
35. Lee H, Kang S, Kim SC, Pui DY. Modeling transport of coloidal particles through polydisperse fibrous membrane filters undes unfavorable chemical and physical conditions. Powder Technol. 2019;355:7-17.
36. Mahmoudi D, Rezaei M, Ashjari J, Salehghamari E, Jazaei F, Babakhani P. Impacts of stratigraphic heterogeneity and release pathway on the transporto f bacterial cells in porous media. Sci Total Environ. 2020;729(138804):1-11.
37. Muneer R, Hashmet MR, Pourafshary P. Fine Migration Control in Sandstones: Surface Force Analysis and Application of DLVO Theory. ACS Omega. 2020;5:31624-39.
38. Ruckenstein E, Prieve DC. Adsorption and desorption of particles and their chromatographic separation. AIChE J. 1976;22(2):276-83.
39. Yang Z, Hou J, Pan Z, Wu M, Zhang M, Wu J, et al. A innovative stepwise strategy using magnetic FE_3O_4-co-graft tannin/polyethyleneimine composites in a coupled process of sulfate radical-advanced oxidation processes to control harmful algal blooms. J Hazard Mater. 2022;439(129485):1-11.
40. Xia T, Li S, Wang H, Guo C, Liu C, Liu A, et al. Insights into the transport of pristine and photoaged graphene oxide-hematite nanohybrids in saturated porous media: Impacts of XDLVO interactions and surface roughness. J Hazard Mater. 2021;419(126488):1-11.

41. Li W, Qi W, Chen J, Zhou W, Li Y, Sun Y, et al. Effective removal of fluorescente microparticles as *Cryptosporidium parvum* surrogates in drinking water treatment by metallic membrane. J Memb Sci. 2020;594(117434):1-10.
42. Xu H, Jiang H, Yu G, Yang L. Towards understanding the role of extracelular polymeric substances in cyanobacterial *Microcystis* aggregation and mucilaginous bloom formation. Chemosphere. 2014;117:815-22.
43. Kwon B, Park N, Cho J. Effect of algae on fouling and efficiency of UF membranes. Desalination. 2005;179:203-14.
44. Yang Y, Hou J, Wang P, Wang C, Wang X, You G. Influence of extrecellular polymeric substances on cell-NPs heteroaggregation process and toxicity of cerium dioxide NPs to *Microcystis aeruginosa*. Environmental Pollution. 2018;242:1206-16.
45. Ren B, Weitzel KA, Duan X, Nadagouda MN, Dionysiou DD. A comprehensive review on algae removal and control by coagulation-based processes: mechanism, material, and application. Sep Purif Technol. 2022;293(121106):1-26.

© 2023 by the authors. Submitted for possible open access publication under the terms and conditions of the Creative Commons Attribution (CC BY NC) license (https://creativecommons.org/licenses/by-nc/4.0/).